International Journal of Biological Macromolecules 284 (2025) 137658

Contents lists available at ScienceDirect

International Journal of Biological Macromolecules

journal homepage: www.elsevier.com/locate/ijbiomac

Development of antioxidant films based on anthocyanin microcapsules extracted from purple corn cob and incorporated into a chitosan matrix

Milagros Sofia Bustamante-Bernedo [a], Lizbet León Félix [a,*], Eduart Gutiérrez-Pineda [b], Nils Leander Huamán-Castilla [c], Jose Luis Solis [d], Mónica Marcela Gómez León [d], I.R. Montoya-Matos [e], J.C. Yacono-Llanos [e], David G. Pacheco-Salazar [a]

[a] Laboratorio de Películas Delgadas y Nanomateriales, Escuela Profesional de Física, Universidad Nacional de San Agustín de Arequipa, Av. Independencia s/n, Arequipa, Peru
[b] Laboratory of Research and Agri-Food Development – LIDA, School of Basic Sciences, Technology and Engineering, National University Open and Distance (UNDA), Bogotá D. C., Colombia
[c] Escuela Profesional de Ingeniería Agroindustrial, Universidad Nacional de Moquegua, Prolongación Calle Ancash s/n, Moquegua 18001, Peru
[d] Universidad Nacional de Ingeniería, Facultad de Ciencias, Av. Tupac Amaru 210, Lima 15333, Peru
[e] Facultad de Ingeniería, Universidad de Lima, Av. Javier Prado Este 4600, Lima 15023, Peru

ARTICLE INFO

Keywords:
Anthocyanins
Purple corn cob
Microencapsulation
Casting
Biodegradable films

ABSTRACT

Biodegradable food packaging films were prepared from chitosan incorporated with microencapsulated anthocyanins powder (MAP) that was extracted from purple corn cob using the casting method. Anthocyanins extracts were microencapsulated with maltodextrin, gum arabic, and soy protein using a spray-drying method. The film based on chitosan and MAP (CHt@MAP) was prepared through citric acid cross-linking and plasticization with glycerol. The structural analysis of the CHt@MAP film revealed a semicrystalline structure by X-ray diffraction. The interactions were mainly via electrostatic and hydrogen bonding, as confirmed by Fourier-transform infrared. Based on scanning electron microscopy, the morphology of the films revealed evidence of the presence of MAP on the surface and cross-section. The microcapsules inside the films produced an increase in thickness (0.18–0.21 mm), lower water vapor permeability (12.4–8.5 $\times$ 10^{-10} g $m^{-1}s^{-1}Pa^{-1}$), and reduced elongation at break (217 % to 165 %), as well as tensile strength (1.3 to 0.45 MPa) compared to the chitosan film. Furthermore, the antioxidant activity of CHt@MAP film was high, with a radical scavenging activity of 56 %. It also exhibited a strong barrier to UV and visible light. The results indicate that the CHt@MAP film preserves the shelf life of blueberries at room temperature and could be used as an active packaging film for foods.

1. Introduction

Food spoilage is a serious concern as it leads to significant economic losses during the transportation and storage of agricultural products, due to environmental factors, handling, and microbial contamination [1]. To address this challenge, the development of packaging with bioactive compounds has emerged as a promising strategy. These active compounds preserve food quality, extend shelf life, and reduce food waste [2].

Purple corn cob (*Zea mays* L.) is a by-product of purple corn that presents a very intense purple color because it is a rich source of anthocyanins (Cy-3-glucoside, Pg-3-glucoside, Pn-3-glucoside, Cy-3-malonylglucoside and Cy-3-dimalonylglucoside) [3,4], as well as other phenolic compounds.

Anthocyanins, a type of flavonoid, are particularly attractive for these applications because of their excellent antioxidant and light barrier properties [5]. However, anthocyanins are susceptible to external factors such as light, oxygen, pH, and high temperatures [6]. Considering the challenges of anthocyanin degradation, microencapsulation emerges as the most effective and scalable solution. This process utilizes various biopolymers as protective "wall materials" to encapsulate the bioactive compounds. Techniques such as spray drying achieve this

* Corresponding author.
E-mail addresses: mbustamantebe@unsa.edu.pe (M.S. Bustamante-Bernedo), lleonf@unsa.edu.pe (L.L. Félix), eduart.gutierrez@unad.edu.co (E. Gutiérrez-Pineda), nhuamanc@unam.edu.pe (N.L. Huamán-Castilla), jsolis@uni.edu.pe (J.L. Solis), mgomez@uni.edu.pe (M.M.G. León), imontoya@ulima.edu.pe (I.R. Montoya-Matos), Jyacono@ulima.edu.pe (J.C. Yacono-Llanos), dpachecos@unsa.edu.pe (D.G. Pacheco-Salazar).

https://doi.org/10.1016/j.ijbiomac.2024.137658
Received 13 May 2024; Received in revised form 10 October 2024; Accepted 12 November 2024
Available online 17 November 2024
0141-8130/© 2024 Published by Elsevier B.V.

encapsulation, which can preserve the properties and ensure the stability and longevity of the bioactive compounds (i.e., the core material) such as anthocyanins [7].

Encapsulation of Anthocyanins with maltodextrin demonstrates optimal effects in preventing degradation due to heat, light, and others forms of degradation [8]. Maltodextrin concentrations from 7 % to 20 % are the most common for spray drying conditions [9]. However, maltodextrin has limitations, particularly regarding its water solubility. To address this issue, proteins and gum arabic can be used as complementary encapsulation materials. While proteins have low solubility in water, they exhibit good film and gel-forming properties and are also used as carriers for the microencapsulation and stabilization of bioactive compounds [10]. Similarly, gum arabic is a water-soluble polymer with low viscosity that has an excellent capability to encapsulate flavors, aromas, phenolic compounds, antioxidants, and nutraceutical compounds [11]. Therefore, it is important to incorporate microcapsules into a polymeric matrix [12]. Chitosan is one of the most well-known polymers because of its excellent film formation, biocompatibility, biodegradability, and antioxidant properties [13]. This polysaccharide dissolves in an acidic medium, such as acetic acid. However, acetic acid releases an unpleasant odor that, if used for packaging, may transfer the smell to the food [14]. For this reason, citric acid was used to prepare the active film because it is an organic compound recognized as safe (GRAS) and is commonly used as a food preservative [15]. At present, microencapsulated anthocyanins incorporated into films are being used for food preservation during storage. The increasing demand for fresh fruit in international markets requires a better solution for fruit preservation. Teixeira et al. reported that chitosan deep eutectic solvent films incorporated with 2 % of açaí microparticles exhibited the most desirable combination of mechanical and antioxidant properties, thus making it a promising material for use in food packaging [16]. Although several studies have investigated the use of films containing bioactive compounds to extend the shelf life of foods, the use of anthocyanin microcapsules extracted from purple corn cob as an alternative to enhance the antioxidant and preservative potential of biodegradable films has not been investigated.

Therefore, this study aimed to develop and characterize the effect of incorporating microencapsulated anthocyanins powder from purple corn cob on the food packaging properties of biodegradable chitosan films. The films were obtained by casting method, and the structure, morphology, physical and barrier properties, antioxidant properties and biodegradability of the films were studied and compared with the chitosan film without microcapsules. Additionally, the potential of these films in fresh blueberries packaging was evaluated, aiming to preserve their shelf life while maintaining quality.

2. Material and methods

2.1. Material

The raw material was purple corn cob (Z. Mays L) that was collected directly from a local market (Arequipa, Perú). Citric acid anhydrous (Scharlau), high molecular weight chitosan (75 % deacetylation) was purchased from Sigma-Aldrich, maltodextrin (MD) with a dextrose equivalent (DE = 10–15), soy protein (purity ≥90 %), and gum arabic (GA) were purchased from Oregon Chem Group (Lima, Perú). All reagents were of analytical grade.

2.2. Extraction of anthocyanin from purple corn cob

Dry purple corn cobs were manually cleaned to remove soil and then dried in a drying oven at 30 °C. Next, they were ground into a powder using a mill (ML G201, GRINDER), and the powder was sifted through 100-mesh sieve. Samples were stored in amber glass bottles until further use.

For the extraction process, 10 g of purple corn cob powder was added to 200 mL of an acidified solution of 60 % ethanol in water. The pH of this solution was adjusted to 2.0 using a 1 M citric acid solution. This solution was maintained in an ultrasonic bath (EMAG UC-20 SD, Germany) at 45 kHz and 120 W for 1 h. The solution was then stirred for 1 min and filtered using a semi-slow filter paper (7-um) to collect the anthocyanin extract. The anthocyanin extract was then concentrated using a rotary evaporator (RE100-PRO, DLAB, China) at 40 °C for 1 h to remove organic solvents. Finally, the concentrated purple corn cob extract (PCCE) was stored in amber glass bottles under refrigerated conditions (10 °C) until further use.

2.3. Preparation of anthocyanins microcapsules

The encapsulation process of PCCE included a spray-drying method utilizing maltodextrin MD, soy protein (SP), and GA as the wall material. The microencapsulation process began with a mixture of matrices each one at (10 % *w/v*). Initially, 10 g of MD was dispersed into 100 mL of distilled water and stirred magnetically for 1 h. Next, the MD solution was mixed with 10 g of SP for 1 h, and finally, 10 g of GA was added and mixed for another 1 h. Each matrix was subject to continuous stirring at 500 rpm and room temperature. After that, the matrix solution was maintained at rest for 12 h. Furthermore, 100 mL of the concentrated anthocyanin extract was added to the coating material suspension as wall material (10:3, *v/w*) under constant stirring at 700 rpm for 3 h. The total soluble solid content of the mixture was 20° Brix.

The resultant solutions were fed into the primary chamber through a peristaltic pump at room temperature under continuous stirring. The drying process was performed in a Mini Spray Dryer (Model B-290, Buchi, Switzerland). The spray dryer was operated with an inlet temperature of 160 °C and an outlet temperature of 90 °C ± 5 °C, with a feed rate of 4.8 mL/min, a drying air flow rate of 538 L/h, nozzle diameter of 0.7 mm, and an aspiration rate of 75 %. The process was performed in triplicate. The obtained microencapsulated anthocyanin powders (MAP) were vacuum sealed and stored in a desiccator at 23 °C and 28 % relative humidity (RH) for further physicochemical analyses.

2.4. Preparation of active films

The solution casting method was used to prepare the films. A chitosan solution (2 wt%) was added to 100 mL of citric acid solution (2 % *w/v*). The mixture was stirred at 500 rpm for 5 min and sonicated for 8 min (2 min on and 1 min off sequentially) using a sonotrode S24d22D and 240 W (HIELSCHER ultrasonic homogenizer, 24 kHz, model UP400ST) to disrupt the particle agglomerates. This mixture was then degassed for 30 min to obtain a homogeneous filmogenic solution. After cooling to 35 °C, 2 g of anthocyanin microparticles were added to the filmogenic solution as previously described. The mixture was placed in an ultrasonic homogenizer for 2 min and stirred magnetically for another 15 min. Thereafter, 2 mL of glycerol was added to the mixture and thoroughly mixed for 30 min, followed by degassing for 20 min.

The resulting solutions were cast onto a plastic petri dish (150 × 20 mm) and dried in a drying oven at 30 °C (MEMMERT, model UF75) for 16 h. The chitosan film (CHt film) with anthocyanin encapsulated (CHt@MAP) was stored in a desiccator at an RH of 28 % for several weeks before analysis.

2.5. Characterization of extract and microcapsules

2.5.1. Total anthocyanin content

The total anthocyanin content (TAC) was evaluated using the pH differential method described by Giusti and Wrosltad [17] and calculated using Eq. (1).

$$TAC(mg/L) = \frac{A \times MW \times DF \times 1000}{\varepsilon \times L} \quad (1)$$

where A equals (Abs530nm − Abs700nm) $_{pH\ 1.0}$ − (Abs530nm − Abs700nm) $_{pH\ 4.5}$, MW is the molecular weight of cyanidin-3-glucoside (C3G) (449.2 g/mol); DF is the total dilution factor of the sample; ε is the molar extinction coefficient of C3G (26,900 L/(mol^{-1} cm^{-1})); and L is the path length of the cuvette (1 cm).

2.5.2. Encapsulation efficiency

The encapsulation efficiency (EE) of the microcapsules was calculated using Eq. (2), as described by Zhang et al. [18], with modifications to the process. Initially, 100 mg of microcapsules were mixed with 1 mL of distilled water and extracted in an ultrasonic bath for 30 min. Then, 9 mL of ethanol was added, and the microcapsules were filtered after 10 min. The resulting mixtures were analyzed to calculate the TAC. To determine the surface anthocyanin content (SAC) of the microcapsules, 100 mg samples were mixed with 10 mL of ethanol, vortexed, centrifuged, and the supernatant was collected and filtered.

$$EE(\%) = \frac{TAC - SAC}{TAC} \times 100, \tag{2}$$

2.5.3. Moisture content and drying yield of the microcapsules

The moisture content percentage in the microcapsules was determined using a humidity balance (MB120, OHAUS, USA). In addition, the drying yield percentage was evaluated using Eq. (3) [19].

$$Drying\ yield\ (\%) = \frac{powder\ after\ spray\ drying(g)}{solids\ in\ feed\ solution(g)} \times 100 \tag{3}$$

2.5.4. Total phenolic content (TPC) and oxygen radical absorbance capacity (ORAC) analysis to determine antioxidant capacity

The total polyphenol content (TPC) and antioxidant capacity of PCCE and MAP were calculated using the method detailed by Huamán-Castilla et al. [20], with a preliminary treatment used for the extraction of TPC and antioxidant compounds from MAP. For TPC, 0.2521 g of sample powder was dissolved in 5 mL of distilled water, stirred for 2 min, and stored in the dark for approximately 1 h. Subsequently, the supernatant was filtered using Whatman Filter Paper Grade 42 and collected in a falcon tube for further analysis. The TPC samples were then evaluated using a UV–vis spectrophotometer (Genesys 150, Thermo Scientific) at 765 nm and expressed as the gallic acid equivalent (GAE) per g of dry weight, utilizing a standard curve of gallic acid (20 mg/mL − 80 mg/mL; r2: 0.9995).

For the ORAC analysis, 0.5 g of sample powder was dissolved in 50 mL of distilled water, followed by the prior extraction of anthocyanins from MAP. The results were represented by plotting the fluorescence values against time and integrating the area under the curve. Trolox calibration curves with known concentrations were used to convert the area under the curve to Trolox equivalents. The antioxidant capacity was expressed as μmol Trolox equivalents per gram of dry weight.

2.6. Characterization of the active film

2.6.1. Chemical structures

The X-ray diffraction (XRD) pattern of the prepared film samples was measured using a Rigaku MiniFlex 600 X-ray) diffractometer operated at 40 kV and 15 mA with Cu Kα radiation (α = 1.5418 Å). Diffractograms were captured between 5 and 60° at a scan speed of 2°/min with a step size of 0.02.

Identification of the different functional groups on the film surface and the interaction between polymers was obtained using a Fourier-transform infrared (FTIR) spectrophotometer (Shimadzu IRTracer-100 Model) in attenuated total reflectance (ATR) mode. The analysis was performed with a resolution of 2 cm^{-1} in the wavenumber range of 4000–400 cm^{-1} with a total of 32 scans.

2.6.2. Surface morphology

Surface morphology and cross-sections of the films were evaluated using a Thermo Scientific Scios 2 DualBeam microscope. The prepared samples were deposited on carbon conductive tape and coated with a thin layer of gold. An accelerating voltage of 15 kV was used during the experiments.

2.6.3. Thickness and moisture content

The film thickness was measured at six random positions using a Mitutoyo digital micrometer (0.001 mm). In addition, the moisture content was determined using the humidity balance described above.

2.6.4. Optical properties

A film sample was cut into 3.5 × 1 cm pieces and placed in a cuvette cell within a UV–vis spectrophotometer (Shimadzu, UV-1800, Japan) to determine its optical properties. The film opacity was measured using Eq. (4).

$$Opacity = \frac{Abs_{600}}{x} \tag{4}$$

where Abs600 is the absorbance value of film at 600 nm and x is the value of the film thickness (mm) that was measured with the digital micrometer as described above.

2.6.5. Water vapor permeability

The water vapor permeability (WVP) of the films was performed according to the method previously described by Quequezana-Bedregal et al. [21]. Vials containing 1 mL of an oversaturated potassium nitrate solution were sealed with film samples and maintained in a desiccator (24.23 °C, 44.89 % HR). The WVP was measured in g m^{-1} s^{-1} Pa^{-1} and calculated using Eq. (5).

$$WVP = \frac{WVPR \times z}{P \times \Delta RH} \tag{5}$$

where the WVP rate (WVPR) is calculated as the slope/film area, P is the water vapor pressure (Pa), ΔRH is the difference in RH, and z is the film thickness (m).

2.6.6. Mechanical properties

Tensile strength (TS), elongation at break (EB), and Young's modulus (YM) properties were determined according to the ASTM D882-02 standard method using a universal testing machine (Testometric X500–50). The films were cut into rectangular strips (1 × 10 cm) and kept in a desiccator with a constant temperature of 25 °C and an RH of 50 % ±5 % for 48 h before testing. The tests were performed with a crosshead speed of 30 mm/min and an initial grip separation of 50 mm, in accordance with the ASTM D882-02 standard method for all experiments.

2.6.7. Biodegradation test

The film's biodegradation was evaluated according to the method described by Chavez-Marquez et al. [22]. The films were cut into 2 × 2 cm squares and placed inside a 10 × 20 × 5 cm cell, buried approximately 1 cm deep in commercial compost. The cell was maintained at room temperature, and films were carefully removed every 1, 2, and 3 days. Before visual inspection of the buried films, the samples were washed and dried at 25 °C.

2.6.8. Antioxidant activity of films

The DPPH radical scavenging activity (RSA) was performed according to the method described by Miao et al. [23] and was calculated using Eq. (6). Approximately 0.5 g of the films were dissolved in 50 % ethanol and vortexed (Vortex Vib J.P. Selecta) for 2 min. Subsequently, 50.7 μM of DPPH solution (3 mL) was combined with the solubilized film (1 mL) and stored in the dark for 30 min.

$$RSA\% = \frac{(A_{DPPH} - A_{sample})}{A_{DPPH}} \times 100. \quad (6)$$

2.7. Evaluation of CHt@MAP films for the enhanced preservation of blueberries

CHt and CHt@MAP films were cut into 10 × 4 cm rectangles and sealed in bags using a heat sealer (FreshpackPro, QH-01, China). Approximately 2 g of fresh blueberries with a small size, maturity, and no damage were used for the test. The bags were stored at room temperature of 25 °C ± 3 °C and an RH of 54 % for 32 days.

Furthermore, the weight loss of blueberries was determined every 2 days during the first week and then every 3 days thereafter. An OHAUS PX225D analytical balance (±0.0001 g) was used, and the results were expressed as a percentage of weight loss relative to the initial sample weight. The packaging tests were performed in triplicate, and the average results were reported.

$$Weight\ loss(\%) = \left(\frac{W_O - W_f}{W_O}\right) \times 100, \quad (7)$$

where W_O is the initial weight and W_f is the weight after the established time.

2.8. Statistical analysis

Experimental data were processed using statistical software (Minitab, 18). The Student's *t*-test was used to determine differences at a 95 % significance level. All data were expressed as the mean ± standard deviation of the analyses performed in triplicate.

3. Results and discussion

3.1. Characterization of the extraction and microencapsulation of anthocyanin

The TAC of the PCCE was 24.5 ± 0.2 mg/g dry weight and was quantified in terms of C3G as the main component in purple corn cob [24] from Arequipa [25].

The MAP was obtained through the spray-drying method by combining three types of wall materials (MD, SP, and GA). The feed solution was prepared with a total soluble solid content of approximately 20° Brix. The concentration of the carrier agent played an important role [9] in increasing the dry yield (61 ± 5 %) and reducing the moisture content (3.5 ± 0.3 %) of the microcapsules. The EE percentage of anthocyanin with wall materials was 97 ± 2 %. These results demonstrate that the composition and relation of the wall material to bind anthocyanin, as well as the core:wall ratio, influence the microencapsulation efficiency. In addition, the drying temperature did not affect the recovery of the bioactive compound. Moreover, several studies have shown that combining polysaccharides with proteins can increase their stability, preservation, and protection properties [26], as well as enhance the efficiency [27,28] of encapsulated bioactive compounds [10,29] due to their ability to change the hygroscopic and thermoplastic characteristics of the powder [30].

3.2. TPC and antioxidant capacity of PCCE and MAP

The antioxidant capacity and phenolic content in PCCE before microencapsulation were 1537 ± 25 μM T.E./dw and 71 ± 1 mg GAE/g dw, respectively. Notably, the TPC of PCCE was higher than the previously reported value of 58.1 mg/g cob [26]. This indicates the ability of PCCE to neutralize free radicals and its phenolic compound concentration per unit of dry weight.

MAP exhibited an antioxidant capacity and phenolic content of 159 ± 5 μM T.E./dw and 1565 ± 0.1 mg/100 g of microsphere, respectively. Moreover, the TPC of the MAP was notably higher than that of microcapsules obtained by spray-drying [19] and freeze-drying [31], suggesting that the microencapsulation process was more effective than previous methods in preserving or enhancing phenolic content and antioxidant capacity. It is crucial to encapsulate natural antioxidants with high TPC and antioxidant capacity and incorporate them into film packaging to increase the shelf life of fresh foods vulnerable to oxidation [32].

3.3. Structural characterization

3.3.1. XRD

Fig. 1 shows the XRD patterns used to analyze the crystal structure of the dry PCCE, MAP, and CHt@MAP films. The XRD pattern of PCCE exhibited the dominance of an amorphous pattern with a wide diffraction peak around 24°. After PCCE microencapsulation, it was observed that the wall materials used had an impact on the crystallinity, which resulted in a semicrystalline structure with a broad main peak around 19°. These changes in the structure may be associated with physical or chemical interactions among the molecules of the wall materials and the bioactive compounds [33], which likely occurred during the spray-drying process.

Conversely, the initial chitosan powder exhibited a crystalline structure with diffraction peaks at approximately 10° and 20°. However, processing the chitosan powder into films resulted in a semicrystalline state, as evidenced by diffraction peaks at approximately 8.9° and 19.6° (data shown in the supplementary material). Moreover, the intensity of the semicrystalline peaks of the chitosan film was not affected by the addition of MAP and exhibited a broad main peak around 19.7°, suggesting a chemical interaction between chitosan and the MAP.

It has been reported in other studies that the crystalline structure of microcapsules impacts their storage stability, which is an important factor in the food industry [34,35]. In addition, during storage, films with a higher crystallinity are less hygroscopic and soluble than amorphous materials [33,35], which might prolong the time of storage, microstructure collapse, nutritional degradation, and probable microbial growth [35,36].

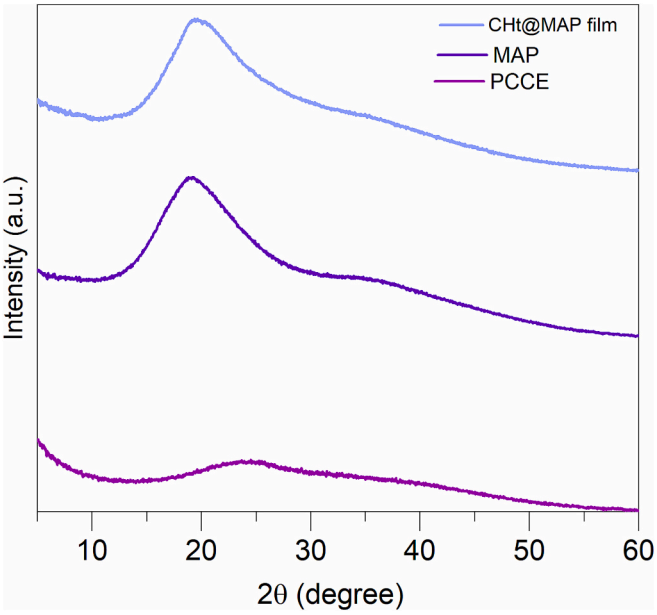


Fig. 1. X-ray diffraction patterns of the purple corn cob extract (PCCE), microencapsulated anthocyanin powder (MAP), and chitosan with MAP (CHt@MAP) films.

3.3.2. FTIR

ATR-FTIR spectroscopy was used to investigate the functional groups and intermolecular interactions between the PCCE and wall materials, as well as the application of MAP in CHt films. Fig. 2 depicts the spectral analysis of the PCCE, which revealed a broad band at 3314 cm^{-1} because of the stretching vibration of hydroxyl groups (O—H bonds) [37,38] that are present in the phenolic groups of the flavonoid molecule [39,40] and water, while the small bands between 2980 and 2903 cm^{-1} are related to the C—H bond stretching vibrations of the flavonoid aromatic phenyl ring [41]. The strong band at 1643 cm^{-1} is related to the stretching vibration of the C═C bond in the aromatic benzenoid ring structure of anthocyanin [42], while the band at 1452 cm^{-1} indicates a C═C bond deformation vibration of phenolic groups [43] or a skeleton vibration of the heterocyclic benzopyran ring in the anthocyanins [44]. The two bands at 1385 cm^{-1} and 1225 cm^{-1} are associated with the interaction between the O—H angular deformation and C—O stretching in phenolics [45], while the band at 1274 cm^{-1} is related to the stretching of the flavonoid pyran rings (C=O) [46]. The band at 1085 cm^{-1} was attributed to the stretching vibration of the C—O ester [46] or C—C rings [47], while the strong band at 1044 cm^{-1} indicates the stretching vibration of the flavonoid C—O esters bond [40]. In addition, the band in the 1000–600 cm^{-1} region indicates the presence of aromatic rings [40].

As shown in Fig. 2, we observed modifications in the FTIR spectrum of MAP. In this sample, a broad band with a reduced intensity at 3314 cm^{-1} suggests a decrease in the O—H stretching vibration, which indicates the formation of a hydrogen bond between flavonoids and wall materials [26], water removal during the spray-drying process, or the presence of carboxylic acids [48] from the wall materials (SP and GA). The broad band that appears at 2929 cm^{-1} indicates free C—H stretching from the carboxylic group of carbohydrates [28,49] because of the overlap of the extracted aromatic band. A lower band observed around 1734 cm^{-1} could represent ester carbonyl groups, suggesting that the carbonyl and amine groups of proteins form hydrogen bonds with the hydrophilic region (hydroxyl group) of anthocyanins [50], resulting in hydrogen bond interaction. The new broad band at 1717 cm^{-1} indicates ester bond C═O stretching vibrations between phenolic present-OH groups of in the extracted anthocyanin and carboxylic acid (-COOH) of proteins or carbohydrates [51]. This chemical interaction provides information regarding the stability of encapsulated anthocyanins. A strong band appearing at 1643 cm^{-1} is related to amide I, which indicates the interaction between anthocyanins and the C—O,

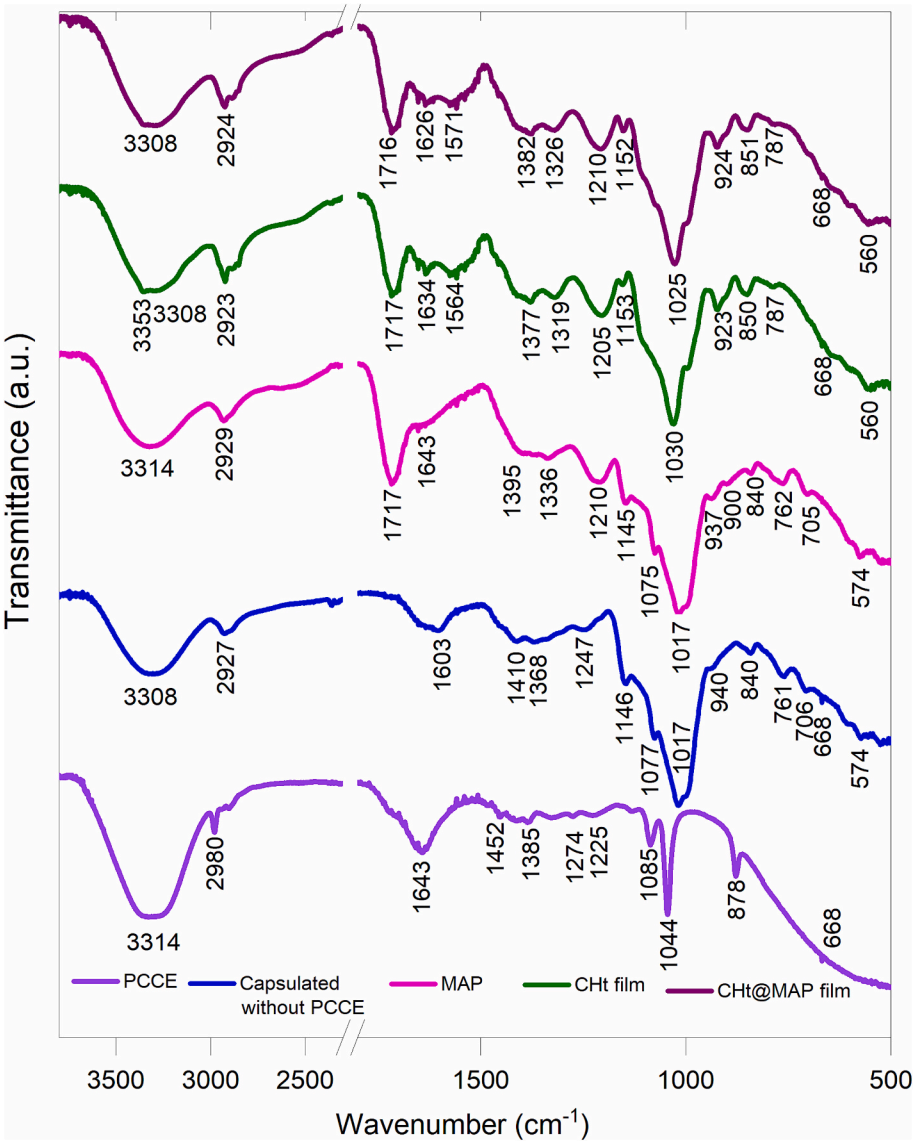


Fig. 2. Attenuated total reflectance-Fourier-transform infrared spectrum of purple corn cob extract (PCCE), capsulated without PCCE, microencapsulated anthocyanin powder (MAP), CHt film, and CHt@MAP film.

C—N, and N—H groups of proteins via hydrophobic attraction [52], electrostatic interaction, or hydrogen bonding [53]. The bands at 1395, 1336, and 1210 cm^{-1} are attributed to the C—O angular deformation of the phenol hydroxyl group [54], or phenolic esters attached to polysaccharides. Furthermore, bands at 1145, 1075, and 1017 cm^{-1} indicate stretching of the C—O bond of carbohydrates [43] and proteins [55]. The bands below 840 cm^{-1} are also present in the wall materials, which suggests that they protect the PCCE during the microencapsulation process. The shift of the band in the amide region may confirm the interaction between phenolic compounds and wall materials, mainly through electrostatic forces [26] or hydrogen bonding [28].

Alternatively, the ATR-FTIR spectrum of the CHt@MAP film exhibited a similar spectrum to that of the CHt film (data shown in the supplementary material), but with a slight shift in the bands. This suggests that the addition of MAP had no significant effect on the chemical structure, as has been reported by similar systems using different biopolymer matrices for encapsulation [33]. The presence of bands at 3353 and 3308 cm^{-1} after the incorporation of the MAP indicates that hydrogen bonds formed between the hydroxyl and amino/hydroxyl groups because of the interaction between the flavonoid and polysaccharides [5,56]. Moreover, similar to the CHt film, C—H stretching vibrations were observed at 2924–2854 cm^{-1}, which indicates that hydrogen bonds may have formed between the chitosan carbon groups and the hydroxyl groups of the polyphenols present in the capsule [51]. A band at 1716 cm^{-1} is attributed to the presence of flavonoids within the microcapsules of the film [51]. In the MAP, the band at 1643 cm^{-1} shifted to 1626 cm^{-1} in the CHt@MAP film, which indicates the presence of electrostatic interactions between the MAP due to phenolic compounds and film [57]. The band at 1571 cm^{-1} is recognized as an amide II (C—N extension and N—H group of the angular change) [58], while bands at 1382, 1326, and 1210 cm^{-1} are related to the N—H and C—N of amide III in the film [58,59]. This shifted band, from 1395 to 1336 cm^{-1} also indicates electrostatic interactions between the MAP and film. The bands at 1152 and 1025 cm^{-1} are related to the elongation length of the glycosidic chain in the saccharin structures because of the MAP addition into the film [51].

3.4. Morphological characterization

Fig. 3(a) shows a scanning electron microscopy (SEM) image of the morphology of MAP, which exhibits a regular and irregular spherical shape with a dented surface. The formation of this shrinkage on the surface of the microcapsule particles could be related to the loss of moisture during the cooling of the drying process. In addition, particle agglomeration is observed, possibly resulting from the inherent stickiness of the encapsulating material. Statistical analysis of the images, using log-normal functions to fit the particle size distribution, revealed a mean size diameter of 8.83 μm and a polydispersity of 0.32 for the microcapsules.

Fig. 3(b) shows SEM images of the CHt@MAP film surface; Fig. 3(c) shows a cross-section of the CHt@MAP film; and Fig. 3(d) presents a magnification image of the cross-section region. In general, several MAP particles were observed dispersed on the surface and within the cross-section of the CHt@MAP films. The appearance of MAP in the film

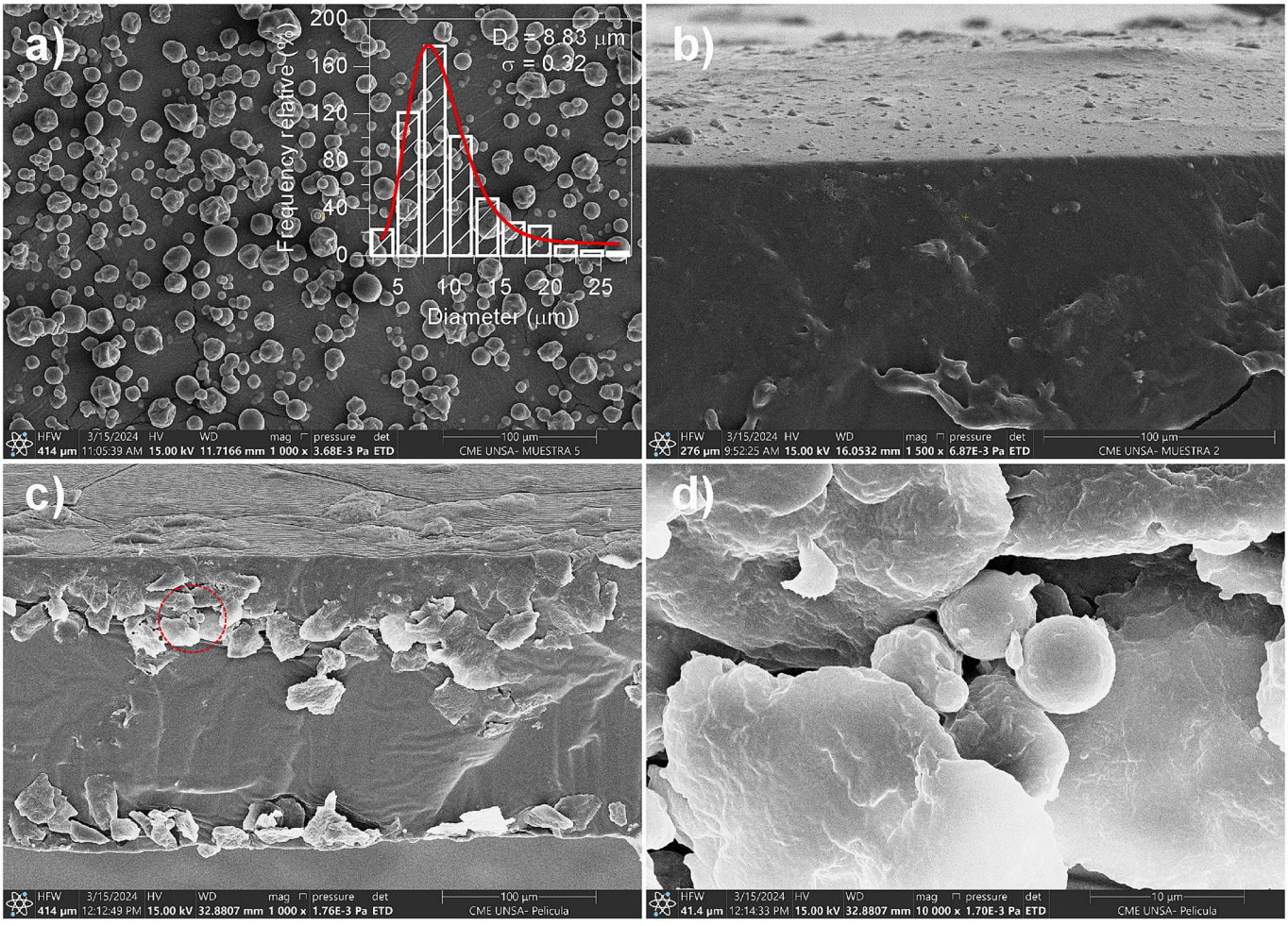


Fig. 3. Scanning electron microscopy image of the microencapsulated anthocyanin powder (MAP) and their particle sizes histogram (a), surface and cross-section of chitosan with MAP (CHt@MAP) films (b and c), and a magnification of image c (d).

could indicate successful incorporation with chitosan. In addition, the films exhibited a uniform thickness of 0.203 mm, a similar value was obtained when using the micrometer, and no cracks were observed in the films.

3.5. Film thickness and moisture content

Film thickness analysis revealed a considerable increase (from 0.18 ± 0.02 mm to 0.21 ± 0.02 mm) after incorporating 2 wt% of MAP into the CHt film. This increase may be attributed to the space occupied by the MAP and swelling of the wall material granules, which subsequently increases the film's thickness and can disrupt the inner structure of the film. In addition, the cross-section SEM images confirmed the presence of MAP in the films.

Moreover, the addition of MAP significantly decreased the moisture content of the CHt film from 11.2 ± 0.3 % to 9 ± 1 %. The reduction of moisture content in the CHt@MAP film could be attributed to the decreased amount of free hydroxyl groups in the film [56,60], thus reducing the water uptake capacity of the film. In addition, the storage conditions (as RH and light) can also impact the moisture content of the films, while the film thickness is an important parameter as it directly influences the opacity, WVP, UV–vis light barrier properties, as well as the mechanical properties of the films.

3.6. Optical properties

Film transmittance and opacity were evaluated based on their ability to block UV–vis light because it can substantially damage food products by causing oxidation or the degradation of nutrients [33,61]. Therefore, a UV–vis light barrier is a desirable property of food packaging films.

Fig. 4 shows that the CHt film without bioactive components exhibited high light transmittance within the UV–vis range, likely because of a lack of UV–vis absorption groups [60]. As a result, the CHt film offers minimal UV–vis light barrier protection.

However, the UV–vis light barrier ability of CHt@MAP films was enhanced through the incorporation of MAP, which is related to the aromatic rings in the anthocyanin structure (e.g., C═C and C═O) that can efficiently absorb UV–vis light [5,62]. Notably, CHt@MAP films completely blocked UV light in the range of 200–350 nm, which is attributed to the abundant aromatic rings [61] present in the polyphenol [63], phenolic, and flavonoid structures [33,64]. In addition, CHt@MAP films exhibited a significantly heightened light barrier, extending the light range from 350 to 550 nm, accompanied by a notable decrease in light transmittance approximately 550 nm, which was correlated with the increased anthocyanin content in the films [65].

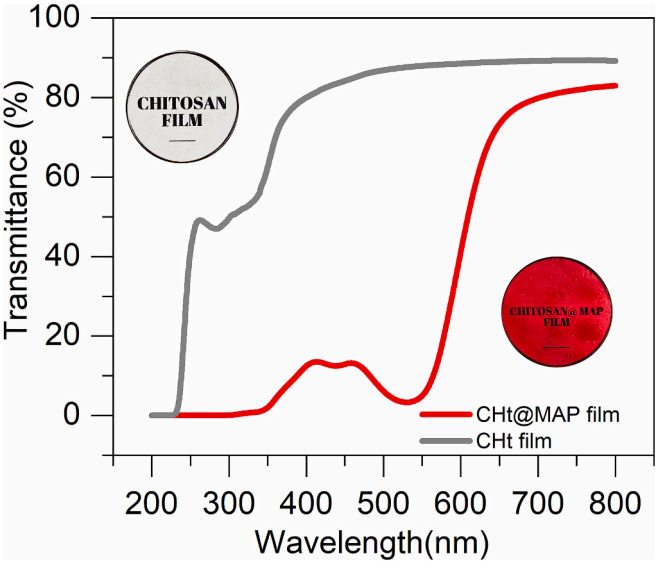


Fig. 4. UV–vis light transmittance of chitosan (CHt) and CHt with microencapsulated anthocyanin powder (CHt@MAP) films and an inset of the physical appearances of the films.

Moreover, the inset photographs in Fig. 4 show the reduced transparency of the CHt films upon the incorporation of the capsulated anthocyanins, which results in a dark red color. This is reflected in the opacity measurement, where the CHt@MAP films show a significantly higher opacity compared to the pure CHt film (0.56 and 2.6 mm at 600 nm absorbance, respectively). Furthermore, the opacity of the CHt films is a parameter that is influenced by the type of acid used and the percentage added, where more opaque films are obtained from the addition of a 5 wt% acid solution [66]. Opacity is an important parameter to consider in food packaging films for consumer acceptance.

In addition, the CHt@MAP films demonstrated excellent color stability when stored at room temperature, whereas the unencapsulated anthocyanins in films often fade over time during storage [5]. These results suggest that CHt@MAP films have excellent barrier properties in the UV–vis region (below 530 nm) and could be used to protect food against quality loss and extend its shelf life.

3.7. Water vapor permeability (WVP)

Normally, food packaging applications require a low WVP of the films to minimize moisture transfer between the food and environment [67], thereby inhibiting chemical and microbial degradation of the food [64] and avoiding the dehydration of fresh produce [68].

The WVP value of the CHt films was significantly higher than those reported for chitosan casting films prepared using different organic acids (2.6 to 6.9 × 10^{-10} g m^{-1} s^{-1} Pa^{-1}) [59] and that of the CHt@MAP films (approximately 24 °C and 45 % RH). This high WVP value can be attributed to the presence of a large number of hydroxyl groups in the film's structure [69].

Furthermore, the increased concentration of glycerol-plasticizer in chitosan films increased their WVP values [70–72] because the plasticizer can increase the intramolecular distance within the chitosan films, thereby making them less dense. In addition, glycerol is hydrophilic because of its free hydroxyl groups, which can absorb moisture, which leads to enhanced water vapor transmission [68]. Moreover, the crosslinking of chitosan and citric acid can reduce the availability of free hydroxyl and amino groups within the chitosan structure [73] because of the increased hydrophobic ester groups [74]. Because of this, the effect of glycerol is reduced, and the interaction with water molecules can be challenging, which leads to a decrease in the WVP. However, the WVP of films can be increased by high concentrations of citric acid [74].

The improved WVP in CHt@MAP films may be attributed to the dispersion of capsulated anthocyanins [75], which provides a physical barrier within the films, leading to an increase in the difficulty of water vapor transport because of a more challenging path [64,75].Other factors that can reduce WVP in CHt@MAP films may be attributed to the formation of ordered layers because of the addition of encapsulated anthocyanins that exhibit semicrystalline structures. This is because the crystalline phase creates a greater barrier to the passage of water molecules compared to the amorphous phase in the films [51]. In addition, as confirmed by FTIR analysis, this may be attributed to the formation of hydrogen bonds and electrostatic interactions between biopolymers and the capsulated anthocyanins, which could have a minor impact on reducing the hydrophilic hydroxyl groups in the CHt@MAP films and consequently result in a lower WVP.

Thus, these results (Table 1) suggest that the reduction in WVP of the films was influenced more by the creation of a challenging path because of the addition of encapsulated anthocyanins and their semicrystalline structure than by hydrogen bonds and electrostatic interactions, which hindered the passage of water molecules through the film.

Table 1
Opacity, water vapor permeability (WVP), and mechanical properties (TS, Tensile Strength; EB, Elongation at beak; and YM, Young's modulus) of chitosan (CHt) and CHt with microencapsulated anthocyanin powder (CHt@MAP) films.

Film	Opacity (mm^{-1})	WVP ($\times 10^{-10}$ g $m^{-1}s^{-1}Pa^{-1}$)	TS (MPa)	EB (%)	YM (MPa)
CHt	0.56 ± 0.04	12.4 ± 1.9	1.3 ± 0.3	217 ± 35	0.6 ± 0.1
CHt@MAP	2.6 ± 0.3	8.5 ± 0.6	0.45 ± 0.05	165 ± 45	0.32 ± 0.08

Values are presented as the mean ± standard deviation ($n = 3$ for opacity; $n = 6$ for TS, EB, and YM).

3.8. Mechanical properties

The mechanical behavior of the films was evaluated through the properties of TS, EB, and Young's modulus (YM), which are presented in Table 1.

The CHt film exhibited a large EB (approximately 217 %) and low TS (approximately 1.3 MPa). We used glycerol and citric acid as cross-linkers to enhance the mechanical properties of the CHt films. The low TS and high EB values obtained could be related to a high amount of citric acid [76] within the films, which increases the brittleness of the films [66]. Furthermore, the chemical structure of citric acid with one hydroxyl and three carboxyl groups confers different functionalities. This allows it to act as both a cross-linking agent and a plasticizer [59] when present in excess in the films [73,74,77] or to form hydrogen bonds between the OH groups of chitosan and citric acid, thus reinforcing the film structure [78]. In addition, an increase in the amount of glycerol can lead to a reduction in TS because of the small glycerol molecules that can diffuse between the chitosan chains [70]. This increases the hydrogen bonding with chitosan [79] (as reflected in the FTIR spectra), and an elevated EB [59] can be attributed to an increase in the film's extensibility (increasing the film's elongation) [70], thus enhancing the chitosan polymer chain flexibility or mobility [80].

Meanwhile, the capsule incorporation led to a significant decrease in both the TS (approximately 0.45 MPa) and EB (approximately 165 %) values of the CHt@MAP film when compared to the CHt film data, which are comparable with previous reports that demonstrated TS and EB values of 0.14–0.75 MPa and 12.1 %–124.2 %, respectively [12]. These reductions in values were probably because of the irregular arrangement of capsule agglomerates, which can increase the pore size of the films (as evidenced by the SEM images) [81], and likely contributed to a reduction in the polymer matrix cohesiveness (density) or reduced mobility of chitosan chains [82]. This made the film structure less compact with a discontinuous microstructure, as well as weak intermolecular interactions (electrostatic interactions) between the capsules and chitosan chains, which improved the mobility of polymeric chains and the plasticizing effect. However, the TS value reported in this study is higher than the TS of previously reported food packaging films (TS of approximately 36 kPa) [81].

Furthermore, the YM of the CHt films was close to 0.6 MPa, whereas the CHt@MAP films exhibited a significantly lower value of 0.32 MPa. Thus, the addition of capsules may have caused a less rigid film than that of CHt. In addition, a decrease in the YM value indicates that the films become more flexible with the incorporation of glycerol [68]. Table 2 summarizes the mechanical, barrier, and antioxidant properties of films with antioxidant activity values reported in the literature. The values of the CHt@MAP film obtained in this work are comparable to those reported in the literature, as shown in Table 2.

Moreover, the CHt films have a certain level of crystallinity because of the strong polymer-plasticizer interactions, which remain after the incorporation of the encapsulated anthocyanin, as confirmed by the XRD results. Furthermore, it is reported that a semicrystalline structure provides a higher mechanical strength [87] and a lower toughness [76] in the material.

These results suggest that an excess of citric acid and glycerol cross-linking induces a plasticizing effect in the CHt film, which results in higher chain mobility and leads to a lower TS and increased EB. Meanwhile, the mechanical properties of the CHt@MAP films could be attributed to the excessive aggregates of encapsulated anthocyanins that interrupt the compactness of the film network and weaken the chemical interactions between them.

Table 2
Properties of CHt@MAP film and other films with antioxidant activity from literature.

Property	CHt@MAP Film	Other films with antioxidant activity
Water vapor permeability (WVP) ($\times 10^{-10}$ g $m^{-1}s^{-1}Pa^{-1}$)	8.5	4.2–4.4 [16,51]
Elongation at break (EB) (%)	165	20–200 [12,58,83,84]
Opacity (mm^{-1})	2.6	1.81–2.50 [12,23,61]
Radical scavenging activity (RSA) (%)	56	56–60 [23,85,86]

3.9. Biodegradability of films in vegetable compost

The biodegradation of CHt and CHt@MAP films was qualitatively evaluated based on the time required for the films to degrade when they were exposed to organic vegetable composting soil (Fig. 5). Unfortunately, we were unable to assess the degradation of the films based on weight changes because of the challenge of removing soil residue that adhered to the film. Fig. 5 shows the general change produced on the surface of the CHt and CHt@MAP films when they were collected for analysis each day. After 1 day of testing, changes on the surface of the films, such as holes and color changes, were visually observed, with the most noticeable differences being observed in the CHt@MAP film compared with the CHt film. In the following days, the changes became more noticeable in the films because of the activity of microorganisms [70], which suggests the beginning of the degradation of films. The temperature, moisture, enzymatic activity of microorganisms, and soil composition are the main factors that determine the film's rate of biodegradation [88].

Other studies have reported successful degradation of chitosan and glycerol films after 4 weeks, thus highlighting the importance of the film's glycerol content during the degradation process [70]. However, blackberry particles in starch films did not alter their biodegradation, with nearly complete disintegration observed after 38 days [88]. The degradation of CHt and CHt@MAP films is less than that of previously reported materials, indicating that biodegradability is a characteristic determined by the matrix chemical composition.

3.10. Antioxidant activity of the films

The RSA of the CHt film was 27 %, thus confirming antioxidant activity because of its free radicals and amino groups, which could prevent the generation of reactive oxygen species related to chain reactions [63,86,89]. Furthermore, this is comparable with other reports of chitosan film incorporating citric acid and glycerol. The film showed 29 % antioxidant activity compared to chitosan films that were prepared with other acids, such as acetic acid, which exhibited an antioxidant activity of <20 %.

Meanwhile, the RSA of the CHt@MAP film was 56 %, which is similar to a previous study with tea polyphenol microcapsules that exhibited an RSA of 37 %–58 % [23]. Other films with antioxidant properties presented an RSA of 60 % and preserved strawberries for about 7 days [85]. These results suggest that the CHt@MAP films could

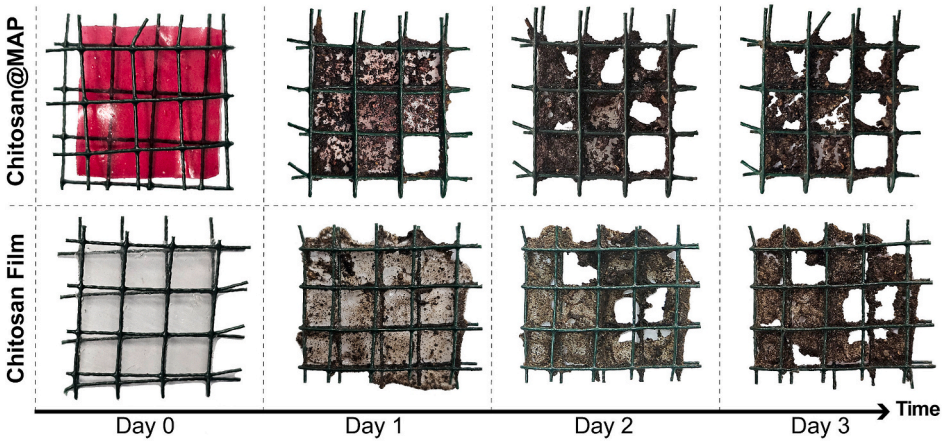


Fig. 5. Photographs of chitosan (CHt) and CHt with microencapsulated anthocyanin powder (CHt@MAP) films showing the degradation variation in organic vegetable composting soil after 3 days.

improve the shelf life of fresh foods.

3.11. Use of CHt@MAP film in fresh blueberries preservation assays

The food packaging potential of the biodegradable CHt and CHt@MAP films was assessed using fresh blueberries, which were stored at room temperature for 5 weeks to simulate the marketing storage conditions. Fig. 6 shows changes in the appearance of the fresh blueberries during the storage period. On the first day, all the blueberries were intact that is, they had a bright dark blue color, a smooth texture, and no wrinkles on the surface. After 1 week of storage, the blueberries packed with the CHt film showed water loss that caused surface wrinkling and the beginning of dehydration. However, the blueberries packed in the CHt@MAP films retained a high moisture content, and no wrinkling was observed. After 2 weeks of storage, the changes in the morphological features of blueberries were more noticeable in samples packaged with theCHt films than in films with the added microcapsules, which indicates quality deterioration of the blueberries (Fig. 6). After 5 weeks of storage, the blueberries packed in CHt films were observed to be almost completely dehydrated, while the blueberries packed in the CHt@MAP films showed only slight changes in appearance. Additionally, the film color did not change during the time of storage.

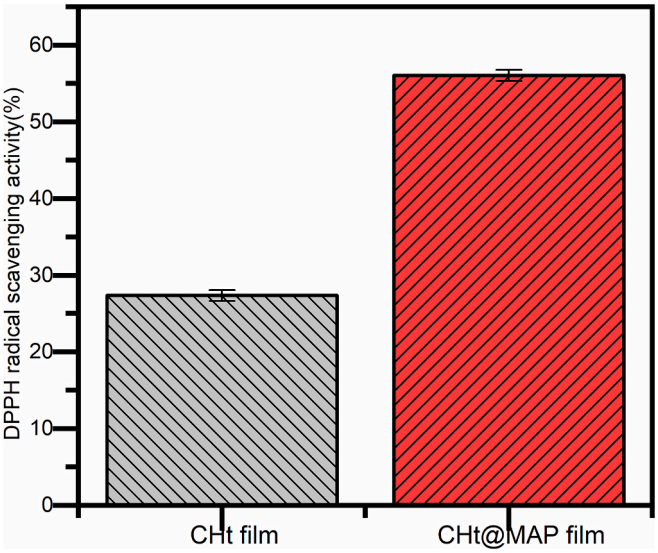


Fig. 6. DPPH radical scavenging activity (%) of chitosan (CHt) and CHt with microencapsulated anthocyanin powder (CHt@MAP) films.

As seen in Fig. 7(b), weight loss is an important indicator for the evaluation of fruit quality. Blueberries packaged with the CHt films exhibit a rapid high weight loss (80 %) during the first 2 weeks of storage, after which it remained constant. Compared with the blueberries packaged with the CHt@MAP films, these films decreased the weight loss of the blueberries with storage time, and the surface state gradually deteriorated, which indicates that this film functioned as a physical barrier to retain water inside the fruit and delayed weight loss. Furthermore, a film with microcapsules reduced the rate of weight loss of strawberries by 49.03 % over 10 days [83], whereas the CHt@MAP films showed a rate of 25 % during the same period (Fig. 7).

At the end of the storage experiment, we found that the water retention of the blueberries packed in the CHt@MAP film was consistent with the low WVP value obtained [73,82] and as a physical barrier to isolate bacteria. This allows for the utilization of the antioxidant and antimicrobial properties of encapsulated anthocyanins and chitosan in food preservation, thereby extending the shelf life of the products.

Furthermore, it reported that the controlled release of capsules embedded within films prolonged the shelf life of fresh blueberries for 7 days [81], whereas our films prolonged freshness for 3 weeks. These results indicate that the incorporation of MAP into biopolymer-based films is a viable approach to developing active packaging to enhance the freshness of fruit. Further research is required to validate the impact of CHt@MAP films on fresh food.

4. Conclusion

The anthocyanin extract from purple corn cob was successfully microencapsulated using MD, GA, and SP isolates as wall materials via spray-drying, achieving an EE of about 96 %. XRD analysis showed that the anthocyanin transitioned from an amorphous to a semicrystalline structure due to the encapsulating matrices. SEM images revealed spherical to semi-spherical particles, some with surface cracking. FTIR analysis indicated successful encapsulation by identifying a new ester band at 1717 cm^{-1}. Active packaging films based on chitosan with incorporated MAP were successfully prepared using the casting method. The CHt@MAP film displayed that their crystallinity did not change after the addition of MAP. ATR-FTIR results indicated that the electrostatic interaction and hydrogen bonding were identified as the main driving forces between MAP and chitosan. The CHt@MAP displayed an improvement in the WVP, UV–vis light barrier ability, and antioxidant activity (an increase from 27 % to 56 %), and a decrease in EB (from 217 % to 165 %) and TS (from 1.3 to 0.45 MPa) compared to the CHt film. This could be related to an excess citric acid and glycerol cross-linking, which causes a plasticizing effect in the CHt film, leading to

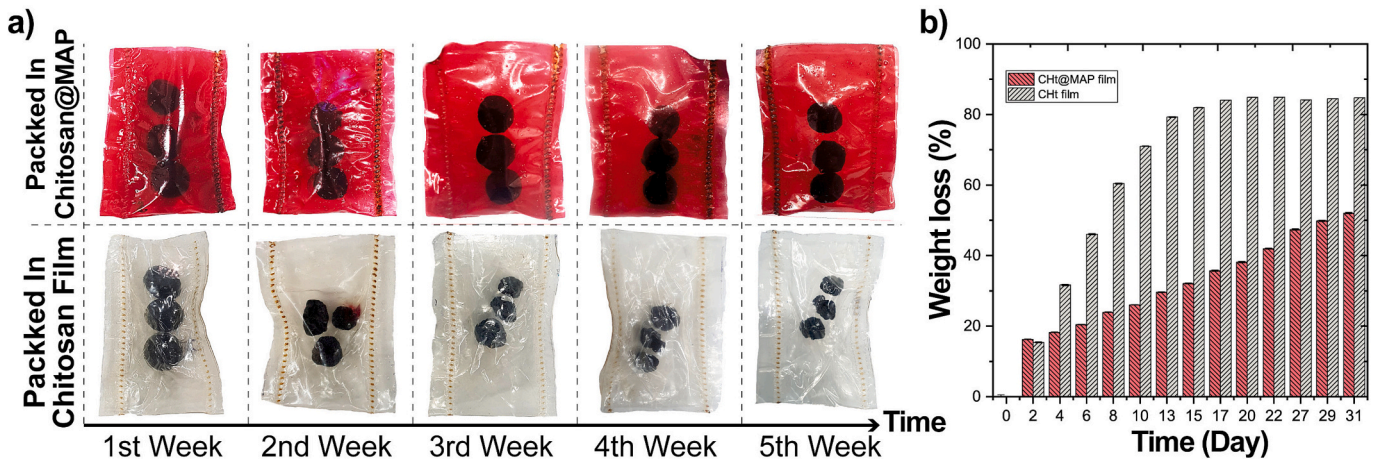


Fig. 7. a) Photographs of blueberries when packed in chitosan (CHt) and CHt with microencapsulated anthocyanin powder (CHt@MAP) films for freshness monitoring of the blueberries and b) weight loss during 32 days of storage.

reduced TS and increased EB. Fresh blueberries packaged in CHt@MAP film preserved 52 % of their weight after 32 days, and the biodegradability test revealed rapid degradation of the films within 3 days. The results of the study suggest that active films hold significant potential for industrial applications in fruit packaging. These films can help lower refrigeration costs while enhancing the safe preservation of fresh fruit products.

CRediT authorship contribution statement

Milagros Sofia Bustamante-Bernedo: Writing – review & editing, Writing – original draft, Validation, Methodology, Investigation, Conceptualization. **Lizbet León Félix:** Writing – review & editing, Writing – original draft, Validation, Supervision, Resources, Project administration, Methodology, Investigation, Funding acquisition, Conceptualization. **Eduart Gutiérrez-Pineda:** Writing – review & editing, Writing – original draft, Validation, Supervision, Investigation, Conceptualization. **Nils Leander Huamán-Castilla:** Writing – review & editing, Writing – original draft, Methodology, Investigation. **Jose Luis Solis:** Writing – review & editing, Writing – original draft, Validation, Investigation. **Mónica Marcela Gómez León:** Writing – review & editing, Writing – original draft, Validation, Investigation. **I.R. Montoya-Matos:** Writing – review & editing, Writing – original draft, Validation, Investigation. **David G. Pacheco-Salazar:** Writing – review & editing, Writing – original draft, Supervision, Investigation.

Declaration of competing interest

The authors declare no competing interests.

Acknowledgments

This work was supported by CONCYTEC through the PROCIENCIA program (contract N° PE501077940-2022-PROCIENCIA).

Appendix A. Supplementary data

Supplementary data to this article can be found online at https://doi.org/10.1016/j.ijbiomac.2024.137658.

References

[1] H. Du, X. Sun, X. Chong, M. Yang, Z. Zhu, Y. Wen, A review on smart active packaging systems for food preservation: applications and future trends, Trends Food Sci. Technol. 141 (2023) 104200, https://doi.org/10.1016/j.tifs.2023.104200.

[2] B. Bayram, G. Ozkan, T. Kostka, E. Capanoglu, T. Esatbeyoglu, Valorization and application of fruit and vegetable wastes and by-products for food packaging materials, Molecules 26 (2021) 4031, https://doi.org/10.3390/molecules26134031.

[3] S.Y. Granados-Balbuena, V. Chicatto-Gasperín, E. Santacruz-Juárez, E. Ocaranza-Sánchez, C. Ramírez-López, M.G. García-Meza, L. Tapia-López, R.R. Robles de la Torre, M.R.R. López, Patented technologies in the extraction, preservation, and application of anthocyanins in food: a review, Appl. Food Res. (2024) 100388, https://doi.org/10.1016/J.AFRES.2024.100388.

[4] G. Rolandelli, L.C. Favre, T.R. Aguirre-Calvo, A.E. Farroni, M. del P. Buera, C. dos Santos Ferreira, An optimized purple corn cob extract as an ingredient for the development of maize-based extrudates with novel characteristics, J. Cereal Sci. 114 (2023) 103809, https://doi.org/10.1016/J.JCS.2023.103809.

[5] H. Yong, J. Liu, Recent advances in the preparation, physical and functional properties, and applications of anthocyanins-based active and intelligent packaging films, Food Packag. Shelf Life 26 (2020) 100550, https://doi.org/10.1016/j.fpsl.2020.100550.

[6] A.G. Tarone, C.B.B. Cazarin, M.R. Marostica Junior, Anthocyanins: new techniques and challenges in microencapsulation, Food Res. Int. 133 (2020) 109092, https://doi.org/10.1016/j.foodres.2020.109092.

[7] M. Jiang, Y. Zhang, Biopolymer-based encapsulation of anthocyanins as reinforced natural colorants for food applications, J. Agric. Food Res. 11 (2023) 100488, https://doi.org/10.1016/j.jafr.2022.100488.

[8] D. Cai, X. Li, J. Chen, X. Jiang, X. Ma, J. Sun, L. Tian, S.K. Vidyarthi, J. Xu, Z. Pan, W. Bai, A comprehensive review on innovative and advanced stabilization approaches of anthocyanin by modifying structure and controlling environmental factors, Food Chem. 366 (2022), https://doi.org/10.1016/j.foodchem.2021.130611.

[9] M.R.I. Shishir, W. Chen, Trends of spray drying: a critical review on drying of fruit and vegetable juices, Trends Food Sci. Technol. 65 (2017) 49–67, https://doi.org/10.1016/J.TIFS.2017.05.006.

[10] Z. Akbarbaglu, S.H. Peighambardoust, K. Sarabandi, S.M. Jafari, Spray drying encapsulation of bioactive compounds within protein-based carriers; different options and applications, Food Chem. 359 (2021) 129965, https://doi.org/10.1016/J.FOODCHEM.2021.129965.

[11] M.R.I. Shishir, L. Xie, C. Sun, X. Zheng, W. Chen, Advances in micro and nano-encapsulation of bioactive compounds using biopolymer and lipid-based transporters, Trends Food Sci. Technol. 78 (2018) 34–60, https://doi.org/10.1016/J.TIFS.2018.05.018.

[12] L. Stoll, T.M.H. Costa, A. Jablonski, S.H. Flôres, A. de Oliveira Rios, Microencapsulation of anthocyanins with different wall materials and its application in active biodegradable films, Food Bioproc. Tech. 9 (2016) 172–181, https://doi.org/10.1007/s11947-015-1610-0.

[13] K. Stefanowska, M. Woźniak, R. Dobrucka, I. Ratajczak, Chitosan with natural additives as a potential food packaging, Materials 16 (2023) 1579, https://doi.org/10.3390/ma16041579.

[14] F. Fernandez-Aulis, L. Hernandez-Vazquez, G. Aguilar-Osorio, D. Arrieta-Baez, A. Navarro-Ocana, Extraction and identification of anthocyanins in corn cob and corn husk from cacahuacintle maize, J. Food Sci. 84 (2019) 954–962, https://doi.org/10.1111/1750-3841.14589.

[15] E. Książek, Citric acid: properties, microbial production, and applications in industries, Molecules 29 (2023) 22, https://doi.org/10.3390/molecules29010022.

[16] B.E. Teixeira-Costa, W.H. Ferreira, F.M. Goycoolea, B.S. Murray, C.T. Andrade, Improved antioxidant and mechanical properties of food packaging films based on chitosan/deep eutectic solvent, containing Açaí-filled microcapsules, Molecules 28 (2023) 1507, https://doi.org/10.3390/molecules28031507.

[17] M.M. Giusti, R.E. Wrolstad, Characterization and measurement of anthocyanins by UV-visible spectroscopy, Curr. Protocol Food Anal. Chem. 00 (2001), https://doi.org/10.1002/0471142913.faf0102s00.

[18] R. Zhang, L. Zhou, J. Li, H. Oliveira, N. Yang, W. Jin, Z. Zhu, S. Li, J. He, Microencapsulation of anthocyanins extracted from grape skin by emulsification/internal gelation followed by spray/freeze-drying techniques: characterization, stability and bioaccessibility, LWT 123 (2020) 109097, https://doi.org/10.1016/j.lwt.2020.109097.
[19] S. Rosales-Chimal, R.O. Navarro-Cortez, L.A. Bello-Perez, A. Vargas-Torres, H. M. Palma-Rodríguez, Optimal conditions for anthocyanin extract microencapsulation in taro starch: physicochemical characterization and bioaccessibility in gastrointestinal conditions, Int. J. Biol. Macromol. 227 (2023) 83–92, https://doi.org/10.1016/j.ijbiomac.2022.12.136.
[20] N.L. Huamán-Castilla, D. Campos, D. García-Ríos, J. Parada, M. Martínez-Cifuentes, M.S. Mariotti-Celis, J.R. Pérez-Correa, Chemical properties of Vitis Vinifera Carménère pomace extracts obtained by hot pressurized liquid extraction, and their inhibitory effect on type 2 diabetes mellitus related enzymes, Antioxidants 10 (2021) 472, https://doi.org/10.3390/antiox10030472.
[21] M. Quequezana Bedregal, E. Medrano de Jara, H. Palza Cordero, L. Miranda Zanardi, Development and characterization of novel packaging films from composite mixtures of rice-starch, tara gum and pectin, J. Food Sci. Technol. 60 (2023) 1153–1162, https://doi.org/10.1007/s13197-023-05669-4.
[22] E. Chavez-Marquez, M.S.B. Bernedo, E.M. de Jara, M.J. Quequezana-Bedregal, E. E. Gutierrez-Oppe, P. de A. Pessôa Filho, Development of intelligent and active potato starch films based on purple corn cob extract and molle essential oil, Int. J. Biol. Macromol. 242 (2023) 125080, https://doi.org/10.1016/J.IJBIOMAC.2023.125080.
[23] Z. Miao, R. Lv, S. Teng, C. Cao, P. Lu, Development of antioxidant active packaging films with slow release properties incorporated with tea polyphenols-loaded porous starch microcapsules, Int. J. Biol. Macromol. 222 (2022) 403–412, https://doi.org/10.1016/j.ijbiomac.2022.09.143.
[24] M. Rabanal-Atalaya, A. Medina-Hoyos, Análisis de antocianinas en el maíz morado (Zea mays L.) del Perú y sus propiedades antioxidantes, REVISTA TERRA LATINOAMERICANA 39 (2021), https://doi.org/10.28940/terra.v39i0.808.
[25] Y.M. Monroy, R.A.F. Rodrigues, A. Sartoratto, F.A. Cabral, Extraction of bioactive compounds from cob and pericarp of purple corn (Zea mays L.) by sequential extraction in fixed bed extractor using supercritical CO2, ethanol, and water as solvents, J. Supercrit. Fluids 107 (2016) 250–259, https://doi.org/10.1016/J.SUPFLU.2015.09.020.
[26] M. Zhao, W. Cao, L. Li, A. Ren, Y. Ang, J. Chen, B. Bhandari, Z. Wang, X. Ren, G. Ren, X. Duan, Effects of different proteins and maltodextrin combinations as wall material on the characteristics of Cornus officinalis flavonoids microcapsules, Front. Nutr. 9 (2022), https://doi.org/10.3389/fnut.2022.1007863.
[27] S. Akhavan Mahdavi, S.M. Jafari, E. Assadpour, M. Ghorbani, Storage stability of encapsulated barberry's anthocyanin and its application in jelly formulation, J. Food Eng. 181 (2016) 59–66, https://doi.org/10.1016/j.jfoodeng.2016.03.003.
[28] M. Mansour, M. Salah, X. Xu, Effect of microencapsulation using soy protein isolate and gum arabic as wall material on red raspberry anthocyanin stability, characterization, and simulated gastrointestinal conditions, Ultrason. Sonochem. 63 (2020) 104927, https://doi.org/10.1016/j.ultsonch.2019.104927.
[29] S. Akhavan Mahdavi, S.M. Jafari, E. Assadpoor, D. Dehnad, Microencapsulation optimization of natural anthocyanins with maltodextrin, gum Arabic and gelatin, Int. J. Biol. Macromol. 85 (2016) 379–385, https://doi.org/10.1016/j.ijbiomac.2016.01.011.
[30] F. Lao, M.M. Giusti, The effect of pigment matrix, temperature and amount of carrier on the yield and final color properties of spray dried purple corn (Zea mays L.) cob anthocyanin powders, Food Chem. 227 (2017) 376–382, https://doi.org/10.1016/j.foodchem.2017.01.091.
[31] A.C. Pereira Souza, P. Deyse Gurak, L. Damasceno Ferreira Marczak, Maltodextrin, pectin and soy protein isolate as carrier agents in the encapsulation of anthocyanins-rich extract from jaboticaba pomace, Food Bioprod. Process. 102 (2017) 186–194, https://doi.org/10.1016/j.fbp.2016.12.012.
[32] V. Chaudhary, N. Thakur, P. Kajla, S. Thakur, S. Punia, Application of encapsulation technology in edible films: carrier of bioactive compounds, Front. Sustain. Food Syst. 5 (2021), https://doi.org/10.3389/fsufs.2021.734921.
[33] J.F. Mendes, L.B. Norcino, A. Manrich, T.J.P. de Oliveira, R.F. Mendes, L.H. C. Mattoso, Pectin-based color indicator films incorporated with spray-dried Hibiscus extract microparticles, Food Res. Int. 162 (2022) 111914, https://doi.org/10.1016/j.foodres.2022.111914.
[34] N.T.N. Hoang, N.N.K. Nguyen, L.T.K. Nguyen, A.T.H. Le, D.T.A. Dong, Research on optimization of spray drying conditions, characteristics of anthocyanins extracted from *Hibiscus sabdariffa* L. flower, and application to marshmallows, Food Sci. Nutr. 12 (2024) 2003–2015, https://doi.org/10.1002/fsn3.3898.
[35] A.A. Mahdi, J.K. Mohammed, W. Al-Ansi, A.D.S. Ghaleb, Q.A. Al-Maqtari, M. Ma, M.I. Ahmed, H. Wang, Microencapsulation of fingered citron extract with gum arabic, modified starch, whey protein, and maltodextrin using spray drying, Int. J. Biol. Macromol. 152 (2020) 1125–1134, https://doi.org/10.1016/j.ijbiomac.2019.10.201.
[36] F. Seke, O.Q. Adiamo, Y. Sultanbawa, D. Sivakumar, In vitro antioxidant activity, bioaccessibility, and thermal stability of encapsulated strawberry fruit (Fragaria × ananassa) polyphenols, Foods 12 (2023) 4045, https://doi.org/10.3390/foods12214045.
[37] B. Bhushan, B. Bibwe, A. Pal, M.K. Mahawar, M.C. Dagla, Y. KR, B.S. Jat, P. Kumar, S.K. Aggarwal, A. Singh, D.P. Chaudhary, FTIR spectra, antioxidant capacity and degradation kinetics of maize anthocyanin extract under variable process conditions, Appl. Food Res. 3 (2023) 100282, https://doi.org/10.1016/j.afres.2023.100282.
[38] J.B. Johnson, A. El Orche, M. Naiker, Prediction of anthocyanin content and variety in plum extracts using ATR-FTIR spectroscopy and chemometrics, Vib. Spectrosc. 121 (2022) 103406, https://doi.org/10.1016/j.vibspec.2022.103406.
[39] S. Thummajitsakul, P. Paensanit, T. Saeieo, J. Sirirat, K. Silprasit, FTIR and multivariate analysis of total phenolic content, antioxidant and anti-amylase activities of extracts and milk of Glycine max L. and Phaseolus vulgaris L, Electron. J. Biotechnol. 64 (2023) 69–75, https://doi.org/10.1016/j.ejbt.2023.04.001.
[40] T.L. Swer, C. Mukhim, K. Bashir, K. Chauhan, Optimization of enzyme aided extraction of anthocyanins from Prunus nepalensis L, LWT 91 (2018) 382–390, https://doi.org/10.1016/j.lwt.2018.01.043.
[41] K. Sakulnarmrat, I. Konczak, Encapsulation of Melodorum fruticosum Lour. anthocyanin-rich extract and its incorporation into model food, LWT 153 (2022) 112546, https://doi.org/10.1016/j.lwt.2021.112546.
[42] E. Safitri, H. Humaira, M. Murniana, N. Nazaruddin, M. Iqhrammullah, N.D. Md Sani, C. Esmaeili, S. Susilawati, M. Mahathir, S. Latansa Nazaruddin, Optical pH sensor based on immobilization anthocyanin from *Dioscorea alata* L. onto polyelectrolyte complex pectin–chitosan membrane for a determination method of salivary pH, Polymers (Basel) 13 (2021) 1276, https://doi.org/10.3390/polym13081276.
[43] L. Favaro, V. Balcão, L. Rocha, E. Silva, J. Oliveira Jr., M. Vila, M. Tubino, Physicochemical characterization of a crude anthocyanin extract from the fruits of Jussara (Euterpe edulis Martius): potential for food and pharmaceutical applications, J. Braz. Chem. Soc. (2018), https://doi.org/10.21577/0103-5053.20180082.
[44] F. Zeng, Y. Ye, J. Liu, P. Fei, Intelligent pH indicator composite film based on pectin/chitosan incorporated with black rice anthocyanins for meat freshness monitoring, Food Chem X 17 (2023) 100531, https://doi.org/10.1016/j.fochx.2022.100531.
[45] L. Resende, L. Oliveira, A. Franca, Polyphenols in Jabuticaba (Plinia spp.) Peel flours: extraction and comparative evaluation of FTIR and HPLC for quantification of individual compounds, Foods 12 (2023) 1488, https://doi.org/10.3390/foods12071488.
[46] K. Zhang, T.-S. Huang, H. Yan, X. Hu, T. Ren, Novel pH-sensitive films based on starch/polyvinyl alcohol and food anthocyanins as a visual indicator of shrimp deterioration, Int. J. Biol. Macromol. 145 (2020) 768–776, https://doi.org/10.1016/j.ijbiomac.2019.12.159.
[47] J. Zhang, X. Huang, J. Shi, L. Liu, X. Zhang, X. Zou, J. Xiao, X. Zhai, D. Zhang, Y. Li, T. Shen, A visual bi-layer indicator based on roselle anthocyanins with high hydrophobic property for monitoring griskin freshness, Food Chem. 355 (2021) 129573, https://doi.org/10.1016/j.foodchem.2021.129573.
[48] E.J.G. Laureanti, T.S. Paiva, L.M. de Matos Jorge, R.M.M. Jorge, Microencapsulation of bioactive compound extracts using maltodextrin and gum arabic by spray and freeze-drying techniques, Int. J. Biol. Macromol. 253 (2023) 126969, https://doi.org/10.1016/j.ijbiomac.2023.126969.
[49] E. Karrar, A.A. Mahdi, S. Sheth, I.A. Mohamed Ahmed, M.F. Manzoor, W. Wei, X. Wang, Effect of maltodextrin combination with gum arabic and whey protein isolate on the microencapsulation of gurum seed oil using a spray-drying method, Int. J. Biol. Macromol. 171 (2021) 208–216, https://doi.org/10.1016/j.ijbiomac.2020.12.045.
[50] J. Song, Y. Yu, M. Chen, Z. Ren, L. Chen, C. Fu, Z. feei Ma, Z. Li, Advancement of protein- and polysaccharide-based biopolymers for anthocyanin encapsulation, Front. Nutr. 9 (2022), https://doi.org/10.3389/fnut.2022.938829.
[51] V.L.C.D. Alves, B.P.M. Rico, R.M.S. Cruz, A.A. Vicente, I. Khmelinskii, M.C. Vieira, Preparation and characterization of a chitosan film with grape seed extract-carvacrol microcapsules and its effect on the shelf-life of refrigerated Salmon (Salmo salar), LWT 89 (2018) 525–534, https://doi.org/10.1016/j.lwt.2017.11.013.
[52] J. Li, B. Wang, Y. He, L. Wen, H. Nan, F. Zheng, H. Liu, S. Lu, M. Wu, H. Zhang, A review of the interaction between anthocyanins and proteins, Food Sci. Technol. Int. 27 (2021) 470–482, https://doi.org/10.1177/1082013220962613.
[53] S. Ren, R. Jiménez-Flores, M.M. Giusti, The interactions between anthocyanin and whey protein: a review, Compr. Rev. Food Sci. Food Saf. 20 (2021) 5992–6011, https://doi.org/10.1111/1541-4337.12854.
[54] G. Espinosa-Acosta, A. Ramos-Jacques, G. Molina, J. Maya-Cornejo, R. Esparza, A. Hernandez-Martinez, I. Sánchez-González, M. Estevez, Stability analysis of anthocyanins using alcoholic extracts from black carrot (Daucus Carota ssp. Sativus Var. Atrorubens Alef.), Molecules 23 (2018) 2744, https://doi.org/10.3390/molecules23112744.
[55] Y. Tao, P. Wang, J. Wang, Y. Wu, Y. Han, J. Zhou, Combining various wall materials for encapsulation of blueberry anthocyanin extracts: optimization by artificial neural network and genetic algorithm and a comprehensive analysis of anthocyanin powder properties, Powder Technol. 311 (2017) 77–87, https://doi.org/10.1016/j.powtec.2017.01.078.
[56] M. Zam, I. Niyumsut, K. Osako, S. Rawdkuen, Fabrication and characterization of intelligent multi-layered biopolymer film incorporated with pH-sensitive red cabbage extract to indicate fish freshness, Polymers (Basel) 14 (2022) 4914, https://doi.org/10.3390/polym14224914.
[57] G. Ren, Y. He, J. Lv, Y. Zhu, Z. Xue, Y. Zhan, Y. Sun, X. Luo, T. Li, Y. Song, F. Niu, M. Huang, S. Fang, L. Fu, H. Xie, Highly biologically active and pH-sensitive collagen hydrolysate-chitosan film loaded with red cabbage extracts realizing dynamic visualization and preservation of shrimp freshness, Int. J. Biol. Macromol. 233 (2023) 123414, https://doi.org/10.1016/j.ijbiomac.2023.123414.
[58] Q.A. Al-Maqtari, A.A.S. Al-Gheethi, A.D.S. Ghaleb, A.A. Mahdi, W. Al-Ansi, A. E. Noman, A. Al-Adeeb, A.K.O. Odjo, Y. Du, M. Wei, W. Yao, Fabrication and characterization of chitosan/gelatin films loaded with microcapsules of Pulicaria

jaubertii extract, Food Hydrocoll. 129 (2022) 107624, https://doi.org/10.1016/j.foodhyd.2022.107624.
[59] A.C. Galvis-Sánchez, A.M.M. Sousa, L. Hilliou, M.P. Gonçalves, H.K.S. Souza, Thermo-compression molding of chitosan with a deep eutectic mixture for biofilms development, Green Chem. 18 (2016) 1571–1580, https://doi.org/10.1039/C5GC02231B.
[60] Y. Qin, Y. Liu, L. Yuan, H. Yong, J. Liu, Preparation and characterization of antioxidant, antimicrobial and pH-sensitive films based on chitosan, silver nanoparticles and purple corn extract, Food Hydrocoll. 96 (2019) 102–111, https://doi.org/10.1016/j.foodhyd.2019.05.017.
[61] D. Thakur, Y. Kumar, V.S. Sharanagat, T. Srivastava, D.C. Saxena, Development of pH-sensitive films based on buckwheat starch, critic acid and rose petal extract for active food packaging, Sustain. Chem. Pharm. 36 (2023) 101236, https://doi.org/10.1016/j.scp.2023.101236.
[62] Y. Qin, F. Xu, L. Yuan, H. Hu, X. Yao, J. Liu, Comparison of the physical and functional properties of starch/polyvinyl alcohol films containing anthocyanins and/or betacyanins, Int. J. Biol. Macromol. 163 (2020) 898–909, https://doi.org/10.1016/j.ijbiomac.2020.07.065.
[63] X. Wang, H. Yong, L. Gao, L. Li, M. Jin, J. Liu, Preparation and characterization of antioxidant and pH-sensitive films based on chitosan and black soybean seed coat extract, Food Hydrocoll. 89 (2019) 56–66, https://doi.org/10.1016/j.foodhyd.2018.10.019.
[64] H. Aloui, A.R. Deshmukh, C. Khomlaem, B.S. Kim, Novel composite films based on sodium alginate and gallnut extract with enhanced antioxidant, antimicrobial, barrier and mechanical properties, Food Hydrocoll. 113 (2021) 106508, https://doi.org/10.1016/j.foodhyd.2020.106508.
[65] D. Yun, H. Cai, Y. Liu, L. Xiao, J. Song, J. Liu, Development of active and intelligent films based on cassava starch and Chinese bayberry (*Myrica rubra* Sieb. et Zucc.) anthocyanins, RSC Adv. 9 (2019) 30905–30916, https://doi.org/10.1039/C9RA06628D.
[66] E. Melro, F.E. Antunes, G.J. da Silva, I. Cruz, P.E. Ramos, F. Carvalho, L. Alves, Chitosan films in food applications. Tuning film properties by changing acidic dissolution conditions, Polymers (Basel) 13 (2020) 1, https://doi.org/10.3390/polym13010001.
[67] C. Tong, Z. Wu, J. Sun, L. Lin, L. Wang, Y. Guo, Z. Huang, C. Wu, J. Pang, Effect of carboxylation cellulose nanocrystal and grape peel extracts on the physical, mechanical and antioxidant properties of konjac glucomannan films, Int. J. Biol. Macromol. 156 (2020) 874–884, https://doi.org/10.1016/j.ijbiomac.2020.04.051.
[68] R. Priyadarshi, Sauraj, B. Kumar, Y.S. Negi, Chitosan film incorporated with citric acid and glycerol as an active packaging material for extension of green chilli shelf life, Carbohydr. Polym. 195 (2018) 329–338, https://doi.org/10.1016/j.carbpol.2018.04.089.
[69] M.J. Bof, F.E. Laurent, F. Massolo, D.E. Locaso, F. Versino, M.A. García, Bio-packaging material impact on blueberries quality attributes under transport and marketing conditions, Polymers (Basel) 13 (2021) 481, https://doi.org/10.3390/polym13040481.
[70] D. Maria V, C. Bernal, N.J. Francois, Development of biodegradable films based on chitosan/glycerol blends suitable for biomedical applications, J Tissue Sci Eng 07 (2016), https://doi.org/10.4172/2157-7552.1000187.
[71] S. Rivero, M.A. García, A. Pinotti, Crosslinking capacity of tannic acid in plasticized chitosan films, Carbohydr. Polym. 82 (2010) 270–276, https://doi.org/10.1016/j.carbpol.2010.04.048.
[72] A.C.S. Oliveira, J.C. Ugucioni, S.V. Borges, Effect of glutaraldehyde/glycerol ratios on the properties of chitosan films, J. Food Process. Preserv. 45 (2021), https://doi.org/10.1111/jfpp.15060.
[73] S. Jiang, C. Qiao, R. Liu, Q. Liu, J. Xu, J. Yao, Structure and properties of citric acid cross-linked chitosan/poly(vinyl alcohol) composite films for food packaging applications, Carbohydr. Polym. 312 (2023) 120842, https://doi.org/10.1016/j.carbpol.2023.120842.
[74] H. Wu, Y. Lei, J. Lu, R. Zhu, D. Xiao, C. Jiao, R. Xia, Z. Zhang, G. Shen, Y. Liu, S. Li, M. Li, Effect of citric acid induced crosslinking on the structure and properties of potato starch/chitosan composite films, Food Hydrocoll. 97 (2019) 105208, https://doi.org/10.1016/j.foodhyd.2019.105208.
[75] A. V., L.S. Badwaik, Recent advancement in improvement of properties of polysaccharides and proteins based packaging film with added nanoparticles: a review, Int. J. Biol. Macromol. 203 (2022) 515–525, https://doi.org/10.1016/j.ijbiomac.2022.01.181.
[76] S. Jiang, C. Qiao, X. Wang, Z. Li, G. Yang, Structure and properties of chitosan/sodium dodecyl sulfate composite films, RSC Adv. 12 (2022) 3969–3978, https://doi.org/10.1039/D1RA08218C.
[77] N. Sharmin, J.T. Rosnes, L. Prabhu, U. Böcker, M. Sivertsvik, Effect of citric acid cross linking on the mechanical, rheological and barrier properties of chitosan, Molecules 27 (2022) 5118, https://doi.org/10.3390/molecules27165118.
[78] R. Poudel, N. Dutta, N. Karak, A mechanically robust biodegradable bioplastic of citric acid modified plasticized yam starch with anthocyanin as a fish spoilage auto-detecting smart film, Int. J. Biol. Macromol. 242 (2023) 125020, https://doi.org/10.1016/j.ijbiomac.2023.125020.
[79] S.E.-D. Al-Mofty, A.H. Karaly, W.A. Sarhan, H.M.E. Azzazy, Multifunctional hemostatic PVA/chitosan sponges loaded with hydroxyapatite and ciprofloxacin, ACS Omega 7 (2022) 13210–13220, https://doi.org/10.1021/acsomega.2c00654.
[80] C. Li, W. Zhu, H. Xue, Z. Chen, Y. Chen, X. Wang, Physical and structural properties of peanut protein isolate-gum Arabic films prepared by various glycation time, Food Hydrocoll. 43 (2015) 322–328, https://doi.org/10.1016/j.foodhyd.2014.06.003.
[81] W. Wang, W. Zhang, L. Li, W. Deng, M. Liu, J. Hu, Biodegradable starch-based packaging films incorporated with polyurethane-encapsulated essential-oil microcapsules for sustained food preservation, Int. J. Biol. Macromol. 235 (2023) 123889, https://doi.org/10.1016/j.ijbiomac.2023.123889.
[82] Z. Yang, X. Zhai, C. Zhang, J. Shi, X. Huang, Z. Li, X. Zou, Y. Gong, M. Holmes, M. Povey, J. Xiao, Agar/TiO2/radish anthocyanin/neem essential oil bionanocomposite bilayer films with improved bioactive capability and electrochemical writing property for banana preservation, Food Hydrocoll. 123 (2022) 107187, https://doi.org/10.1016/j.foodhyd.2021.107187.
[83] D. Hu, Y. Xu, C. Gao, L. Meng, X. Feng, Z. Wang, X. Shen, X. Tang, Preparation and characterization of starch/PBAT film containing hydroxypropyl-β-cyclodextrin/ethyl lauroyl arginate/cinnamon essential oil microcapsules and its application in the preservation of strawberry, Int. J. Biol. Macromol. 259 (2024) 129204, https://doi.org/10.1016/j.ijbiomac.2024.129204.
[84] C.R. Leong, N.S. Daud, W.Y. Tong, S.Y. Cheng, W.N. Tan, N.S. Hamin, K.F. Pa'ee, Gelatine film incorporated with Clitoria ternatea-derived anthocyanin microcapsules, a food packaging material effective against foodborne pathogens, Food Technol. Biotechnol. 59 (2021) 422–431, https://doi.org/10.17113/ftb.59.04.21.7069.
[85] W. Zhao, L. Yu, Y. Gu, W. Ma, K. Wang, J. Liang, Q. Liu, Preparation of dual-functional packaging films containing green tea essential oil microcapsules for strawberry preservation: excellent barrier properties and antioxidant activity, Food Biosci. 56 (2023) 103279, https://doi.org/10.1016/j.fbio.2023.103279.
[86] H. Yong, X. Wang, R. Bai, Z. Miao, X. Zhang, J. Liu, Development of antioxidant and intelligent pH-sensing packaging films by incorporating purple-fleshed sweet potato extract into chitosan matrix, Food Hydrocoll. 90 (2019) 216–224, https://doi.org/10.1016/j.foodhyd.2018.12.015.
[87] C. Qiao, X. Ma, X. Wang, L. Liu, Structure and properties of chitosan films: effect of the type of solvent acid, LWT 135 (2021) 109984, https://doi.org/10.1016/j.lwt.2020.109984.
[88] G. Ferreira Nogueira, F. Matta Fakhouri, R.A. de Oliveira, Incorporation of spray dried and freeze dried blackberry particles in edible films: morphology, stability to pH, sterilization and biodegradation, Food Packag. Shelf Life 20 (2019) 100313, https://doi.org/10.1016/j.fpsl.2019.100313.
[89] Y. Amaregouda, K. Kamanna, T. Gasti, Fabrication of intelligent/active films based on chitosan/polyvinyl alcohol matrices containing Jacaranda cuspidifolia anthocyanin for real-time monitoring of fish freshness, Int. J. Biol. Macromol. 218 (2022) 799–815, https://doi.org/10.1016/j.ijbiomac.2022.07.174.